Economic removal of chlorophenol from wastewater using multi-stage spiral-wound reverse osmosis process: Simulation and optimisation

M. A. Al-Obaidi [1], C. Kara-Zaïtri [2] and I. M. Mujtaba [2, *]

[1] **Middle Technical University, Technical Institute of Baquba, Dayala – Iraq**

[2] **Chemical Engineering, School of Engineering, Faculty of Engineering and Informatics, University of Bradford, Bradford, West Yorkshire BD7 1DP, UK**

***Corresponding author, Tel.: +44 0 1274 233645**

E-mail address: I.M.Mujtaba@bradford.ac.uk

Abstract

The successful use of Reverse Osmosis (RO) process has increased significantly in water desalination, water treatment and food processing applications. In this work, the economic feasibility of a multi-stage RO process including both retentate and permeate reprocessing for the removal of chlorophenol from wastewater is explored using simulation and optimisation studies. Firstly, a mathematical model of the process is developed based on the solution diffusion model, which was validated using experimental chlorophenol removal from the literature, is combined with several appropriate cost functions to form a full model package. Secondly, for a better understanding of the interactions between the different parameters on the economic performance of the process, a detailed process simulation is carried out. Finally, a multi-objective optimisation framework based on Non-Linear Programming (NLP) problem is developed for minimising the product unit cost, the total annualised cost, the specific energy consumption together with optimising the feed pressure and feed flow rate for an acceptable level of chlorophenol rejection and total water recovery rate. The results clearly show that the removal of chlorophenol can reach 98.8% at a cost of approximately 0.21 $/m³.

Keywords: Multi-stage RO Process; Modelling; Simulation; Optimisation; Chlorophenol Rejection; Specific Energy Consumption; Cost Estimation.

1. Introduction

The removal of contaminants from industrial effluents is carried out using a wide range of treatment methods such as UV irradiation, organic solvent extraction, steam distillation processes, adsorption, and membrane technology (Czech and Buda, 2015; Cristale *et al.*, 2016; Carolin *et al.*, 2017). However, the real merit of each treatment method can only be appreciated

if the whole process is achieved at a reasonable total annualised treatment cost. Reverse osmosis (RO) is an established technology for seawater desalination and water reclamation (Uribe *et al.*, 2015; Jiang *et al.*, 2017; Al-Obaidi *et al.*, 2017a, 2018a).

In this respect, RO process has been implemented in several types of industrial applications, where it shows a growth in water recycling and wastewater treatment (Lee and Lueptow 2001; Al-Obaidi *et al.*, 2018b). This is mainly including the effluent treatments of several applications such as (a) dairy industry (Bortoluzzi *et al.*, 2017) (b) textile industry (Amar et al. 2009), (c) pharmaceutical industry (Gholami *et al.* 2012) and (d) tannery industry (George *et al.*, 2015).

RO seawater desalination cost and the efficiency of medium and large-scale plants with optimisation have been considered by many researchers such as Malek *et al.* (1996), Marcovecchio *et al.* (2005), and Sassi (2012). Marcovecchio *et al.* (2005) optimised a large-scale hollow fibre RO seawater desalination system and the production cost was found to be 1.01 – 0.79 $/m³ for a range of operating feed concentration and pressure.

The energy consumption of seawater RO desalination plants is decreased from 20 kWh/m³ in 1970 to around 3.5 kWh/m³ in 1990 and 2.0 kWh/m³ in 2004, where the energy cost of seawater desalination required to drive the high-pressure pumps accounts for around 75% of the total operating cost (MacHarg and Truby, 2004). It is important to note that for brackish water resources, the total energy consumption is in fact below 1 kWh/m³ (Wilf, 2004). Further improvement of water cost production continues with decreasing capital and operating costs. The improvement of membrane elements and pumping system, the proliferation of energy recovery devices, and the optimisation of design and operation are the main contributors to decreasing production cost in the future. In this respect, Sassi and Mujtaba (2013) optimised the design and operation of the seawater RO process considering the variation in water demands and showed that the average daily specific energy consumption in terms of permeate produced varies between 2.397 to 2.774 kWh/m³ in the summer, and 2.647 to 3.044 kWh/m³ in the winter.

Whilst there have been several studies for optimising the design and operation of seawater RO systems, there have been only a few studies which focused on the evaluation of cost efficiency of RO wastewater treatment. Coˆté *et al.* (2005) compared the economic aspects of two ultrafiltration RO plants for seawater desalination and secondary sewage treatment processes. They concluded that the capital and operating costs of seawater process are twice the secondary sewage process costs. Statistically, the total life cycle cost of secondary effluent and seawater

processes are 0.28 $/m³ and 0.62 S$/m³, respectively. This is due to higher operating feed flow rate and pressure of seawater desalination processes. Therefore, it is concluded that there is a significant limitation of the cost functions in the context of RO wastewater treatment processes.

1.1 Novelty and aim of this work

To the best of the authors' knowledge, the evaluation and subsequent optimisation of the total annualized cost and product unit cost of chlorophenol removal from wastewater using the multi-stage RO process has not yet been studied or reported in the literature. Therefore, the main aim of this paper is to develop a methodology for investigating both product unit cost and total annualised cost of the RO wastewater treatment system, and specifically evaluating the performance of retentate-permeate reprocessing design of multi-stage RO process. A commercial multi-stage RO process is proposed for the removal of chlorophenol from wastewater as a result. The proposed design of multistage RO process is based on the combination of the retentate and permeate reprocessing design, which expected to perform high chlorophenol rejection compared to the maximum value of 83% obtained by Sundaramoorthy *et al.* (2011).

Firstly, a model for the individual spiral wound RO module is developed and validated against chlorophenol removal from the literature. Secondly, the model is extended to predict the total chlorophenol rejection, recovery rate, and energy consumption for a multi-stage RO process for the proposed configuration. Thirdly, the model is implemented using a specific set of equations to estimate the total annualised cost of operation and product price unit measured in $/m³. Fourthly, the proposed process is analysed using a simulated study which yields an improved understanding of the interaction between design and operating parameters on the cost of treatment. Finally, the model is incorporated into a multi-objective non-linear optimisation framework to minimise the product unit cost, total annualised cost, and specific energy consumption while optimising the operating conditions of the proposed RO process for a given feed concentration. This final optimisation is constrained with the minimum values of 90% and 50% for chlorophenol rejection and recovery rate, respectively; taking into consideration upper and lower bounds of membrane specifications.

2. Process model

Al-Obaidi *et al.* (2018c) developed a mathematical model for the spiral wound RO membrane to simulate and optimise the rejection of chlorophenol from wastewater. For completeness and the convenience of the readers, their model has been included in Table A.1 in Appendix A. This model has recently been enhanced to improve the estimation of several parameters as explained in the section below.

The mass transfer coefficient of chlorophenol k (m/s) is calculated using Eq. (1), which is estimated by Sundaramoorthy *et al.* (2011) using the linear fit method of experimental data. The mass transfer coefficient equation includes the Reynolds Number in feed Re_f (-) and permeate Re_p (-) channels model and dimensionless solute concentration C_m(-).

$$k = \frac{147.4\, D_b\, Re_f^{0.13}\; Re_p^{0.739}\, C_m^{0.135}}{2\, t_f} \quad (1)$$

$C_m, Re_f,$ and Re_p are defined in Table A.1 in Appendix A.

The retentate pressure $P_{b(out)}$ (atm) is estimated considering the model equation of Al-Obaidi *et al.* (2017b) by assuming the pressure drop, which is quantified by the friction parameter b (atm s/m^4) as illustrated by Darcy's law.

$$P_{f(out)} = \left\{ P_{f(in)} - \left(b\, L\, Q_f\right) + \left(\mathrm{b}\, \mathrm{W}\, \theta \;\; \left(\frac{L^2}{2}\right)\left(\Delta P_{f(out)}\right)\right) - \left[\mathrm{b}^2\, \mathrm{W}\, \theta \;\; \left(\frac{L^3}{6}\right) Q_f\right] - \left[b^2\, W\, \theta \;\; \left(\frac{W\,\theta}{b}\right)^{0.5}\left(\frac{L^3}{6}\right)\left(\Delta P_{f(out)} - \Delta P_{f(in)}\right)\right]\right\} \quad (2)$$

$$\theta = \frac{A_{w(T)}\, B_{s(T)}}{B_{s(T)} + R\,(T + 273.15)\, A_{w(T)}\, C_p} \quad (3)$$

The following equations have been developed to estimate the total recovery rate Rec (-), retentate C_r (kmol/m^3) and permeate concentration C_p (kmol/m^3).

The total mass balance and solute balance of the whole unit gives:

$$Q_f = Q_r + Q_p \quad (4)$$

$$Q_f\, C_f - Q_r\, C_r = Q_p\, C_p \quad (5)$$

$$Q_f\ C_f - Q_r\ C_r - Q_p C_r = Q_p\ C_p - Q_p C_r \quad (6)$$

$$Q_f\ C_f - \ C_r(Q_r + Q_p) = Q_p\ C_p - Q_p C_r \quad (7)$$

$$Q_f\ (C_f - \ C_r) = Q_p(\ C_p - C_r) \quad (8)$$

$$\frac{Q_p}{Q_f} = Rec = \frac{(C_f - C_r)}{(\ C_p - C_r)} \quad (9)$$

The re-arrangement of Eq. (9) yields:

$$C_r = \frac{(C_f - C_p\ Rec)}{(1 - Rec)} \quad (10)$$

$$C_p = \frac{(Q_f\ C_f) - (Q_r\ C_r)}{Q_p} \quad (11)$$

Also, the permeate concentration C_p (kmol/m³) can be written as described in Eq. (12).

$$C_p = \frac{C_f - \frac{Q_r}{Q_f} C_r}{Rec} \quad (12)$$

Finally, a new correlation to calculate the total permeate flow rate Q_p (m³/s) is developed:

$$Q_p = A_{w(T)}\ A\left[\left(\left(P_{f(in)} - P_p\right) - \frac{\Delta P_{drop}}{2}\right) - \left(R\ (T + 273.15)\ exp\left(\frac{J_w}{k}\right)(C_b - C_r(1 - Rej))\right)\right]$$

(13)

The transport parameters of water $A_{w(T)}$ (m/atm s) and chlorophenol $B_{s(T)}$ (m/s) are not constant and vary with the feed concentration and temperature. This is compared to the results of Al-Obaidi *et al.* (2018c), who assumed constant transport parameters. Therefore, Eqs. (14) and (15) are used to illustrate the influence of operating temperature and feed concentration on the transport parameters (Al-Obaidi *et al.*, 2018d).

$$A_{w(T)} = \ A_{w(T_o)}\ \frac{\mu_{b(T_o)}}{\mu_{b(T)}} \quad (14)$$

$$B_{s(T)} = \ B_{s(T_o)}\ \frac{(T+273.15)}{(T_o+273.15)}\ \frac{\mu_{b(T_o)}}{\mu_{b(T)}}$$

(15)

The physical property equations of diluted chlorophenol solution are identical to water equations of Koroneos (2007) and are given in Table A.1 in Appendix A.

2.1 Economic and energy consumption model

The total annual cost (TAC) ($/year) of the RO process consists of total capital cost (TCC) ($/year) and the total operational cost (TOC) ($/year). The capital cost includes equipment, installation, and indirect costs, while the cost related to energy consumption, replacement of

chemicals, and other related costs are included in the operational and maintenance cost. This research focuses on estimating the total annual treatment cost of RO process for the removal of chlorophenol from wastewater. Unfortunately, there is no consistent cost model for estimating water production cost from wastewater, although several attempts have been made and alternative approaches were used in the literature. In this work, the cost model has been developed based on the data used by Malek *et al.* (1996), Marcovecchio *et al.* (2005), Koroneos *et al.* (2007) and Lu *et al.* (2012). The costing model consists of operating and capital costs, and includes wastewater intake and pre-treatment, high-pressure pump, booster pump, and energy recovery device (ERD) costs. This model also incorporates labour and maintenance costs as suggested by Koroneos *et al.* (2007). Interestingly, Malek *et al.* (1996), Marcovecchio *et al.* (2005) and Lu *et al.* (2012) did not take into account labour and maintenance costs in their models. Similarly, this study includes effluents disposal costs, which have not been considered by other similar studies available in the literature. Although the proposed economic models are discussed here in respect of seawater desalination, they can readily be adopted for the modelling of multi-stage RO wastewater treatment process for the removal of chlorophenol.

The total annual cost TAC ($/year) is presented in the Eqs. (16) to (35).

$$TAC = TCC + TOC \quad (16)$$

$$TCC = \left[\left(C_{wwip} + C_{Pump} + C_{ERD} + C_{me}\right) 1.411x0.08\right] \quad (17)$$

$$TOC = OC_{Pu} - OC_{ERD} + OC_{sc} + OC_{ch} + OC_{me} + OC_{lab} + OC_{maint} + OC_{bd} \quad (18)$$

1.411 and 0.08 are the site development and indirect costs and the capital charge rate per annum, respectively (Malek *et al.*, 1996). C_{wwip} ($) represents the wastewater intake and pre-treatment cost, which is estimated using Eq. (19) (Malek *et al.*, 1996).

$$C_{wwip} = 996\ (24x3600\ Q_{f(plant)})^{0.8} \quad (19)$$

The capital cost of high-pressure pump and booster pump C_{Pump} ($) is given in Eq. (20). Eq. (21) shows the capital cost of ERD C_{ERD} ($), which is identical to the capital cost of a high-pressure pump (Lu *et al.*, 2012). These costs are considered as the main components of total

capital cost that affect the price of treatment, where they are estimated based on the total plant feed flow rate as follows.

$$C_{Pump} = \left[52\ (3600\ Q_{f(plant)}\ (P_{f(plant)} 0.101325))^{0.96}\right] + \left[52\ (3600\ Q_{f(stage\_3)}\ (P_{f(Bp)} 0.101325))^{0.96}\right] \quad (20)$$

$$C_{ERD} = \left[52\ (3600\ Q_{f(plant)}\ (P_{f(plant)} 0.101325))^{0.96}\right] \quad (21)$$

It is important to note that the following equations are developed for the suggested RO configuration shown in Fig. 1 and will be described in the next sections. $P_{f(plant)}$, $Q_{f(plant)}$, $Q_{f(stage\_3)}$ and $P_{f(Bp)}$ are the plant pressure, plant volumetric feed flow rate, feed flow rate of stage 3, and the supplied pressure of booster pump, respectively. The membrane module and pressure vessel capital cost C_{me} ($) are mainly dependent on current membrane and pressure vessel prices calculated as follows.

$$C_{me} = N_s\, N_{PV} (C_{ele}\, N_{ele} + C_{PV}) \quad (22)$$

$C_{ele}, C_{PV}, N_s, N_{ele}$, and N_{PV} are the membrane element and pressure vessel cost ($) and the stage, membrane, and pressure vessel numbers, respectively.

The pumping operating cost OC_{pu} ($/year) including the high-pressure pump and booster pump is given in Eq. (23).

$$OC_{pu} = 365x24 \left[\left(\frac{(3600\ (P_{f(plant)}\ 0.101325)\ )\ Q_{f(plant)}\ )}{3.6\ \varepsilon_{pump}\ \varepsilon_{motor}}\right) + \left(\frac{(3600\ (P_{f(Bp)}\ 0.101325)\ )\ Q_{f(Bp)}\ )}{3.6\ \varepsilon_{pump}\ \varepsilon_{motor}}\right)\right] E_c\ L_f \quad (23)$$

Eq. (24) shows the net operating cost of ERD (OC_{ERD} expressed in $/year) (Lu *et al.*, 2012).

$$OC_{ERD} = 365x24 \left(\frac{3600\ \left((P_{f(out_{ERD})}\ 1.01325\right)\ Q_{f(ERD)}}{3.6}\right) E_c\ L_f \quad (24)$$

Therefore, the annual operating net pumping cost OC_{np} is given as shown in Eq. (25).

$$OC_{np} = OC_{pu} - OC_{ERD} \quad (25)$$

$$P_{f(outERD)} = (P_{f(out_{stage})}\, \varepsilon_{ERD})$$

(26)

$$P_{f(Bp)} = P_{f(plant)} - P_{f(outERD)}$$

(27)

E_c ($/ kWh) and L_f (-) are the electricity unit cost and plant load factor per annum, respectively. ε_{pump}, ε_{Bp}, ε_{motor} and ε_{ERD} (-) are the efficiency of high-pressure pump, booster pump, the motor and ERD, respectively. $P_{f(outERD)}$, $P_{f(out_{stage})}$, $Q_{f(ERD)}$ and $P_{f(Bp)}$ are the hydraulic outlet pressure of ERD, retentate pressure of the stage, inlet volumetric flow rate of ERD, which is the same as the concentrate brine stream and operating pressure of the booster pump, respectively. The terms within the main brackets in Eq. (23) and (24) represent the power calculations of the high-pressure and booster pumps power consumption and total energy recovered by turbine ERD (kW), respectively. E_c and L_f are 0.08 and 0.85, respectively and are similar to those used by Marcovecchio *et al.* (2005), Lu *et al.* (2006) and Valladares Linares *et al.* (2016). The energy recovered by the ERD is deduced from the total energy consumption given in Eq. (25) and yields the net pumping cost OC_{np} ($/year). It is interesting to note that the capital cost of the plant is normally increased by 30% as a result of applying the ERD (Franks *et al.*, 2012).

The annual operating spares cost OC_{sc} ($/year), annual chemical treatment cost OC_{ch} ($/year) and effluents disposal cost OC_{bd} ($/year) are calculated using Eqs. (28), (29) and (30), respectively.

$$OC_{sc} = 3600x24x365\, C_{cf}\, Q_{p(plant)}\, L_f \quad (28)$$

$$OC_{ch} = 3600x24x365\, C_{ct}\, Q_{f(plant)}\, L_f$$

(29)

$$OC_{bd} = 3600x24x365\, C_{bd}\, Q_{p(plant)}\, L_f$$

(30)

C_{cf}, C_{ct} and C_{bd} represent the cost of cartridge filters replacement (the replacement rate), cost of chemical treatment and cost of effluents disposal, respectively and are 0.033, 0.018 and 0.0015 $/m³, respectively These costs are around the same values used in the seawater desalination plant analysed by Marcovecchio *et al.* (2005), El-Emam and Dincer (2014) and Al-Obaidani *et al.* (2008). The annual membrane replacement cost OC_{me} ($/year) is calculated using Eq. (31).

$$OC_{me} = 0.2\ C_{me}$$

(31)

The annual labour cost OC_{lab} ($/year) is estimated using Eq. (32) based on Koroneos *et al.* (2007), which is similar to that used for seawater desalination.

$$OC_{lab} = C_{lab}\ 3600x24x365\ Q_{p(plant)}$$

(32)

C_{lab} = 0.02 $/m³ is the labour cost.

The treated water production cost PUC ($/m³), the capital cost recovery factor $CCRF$ (year) and annual maintenance costs (OC_{maint}) ($/year) are estimated using Eqs. (33), (34) and (35), respectively, again all based on Koroneos *et al.* (2007).

$$PUC = \frac{\left(\frac{TCC}{CCRF}\right)+TOC}{3600x\ 24x\ 365\ Q_{p(plant)}}$$

(33)

$$CCRF = \left[\frac{(i+1)^n-1}{i\ (i+1)^n}\right]$$

(34)

$$OC_{main} = 0.02\ PUC\ 3600x24x365\ Q_{p(plant)}$$

(35)

i (-) and n (year) are the discount rate and the plant life, respectively. The useful plant life of 25 years is selected for this research as suggested by Marcovecchio *et al.* (2005). Finally, the total plant specific energy consumption per cubic meter of permeate is influenced by the operating parameters and the osmotic pressure of the process. Specifically, it is calculated based on the consumed energy in the high-pressure pump, booster pump and the recovered energy by the ERD.

$$SEC = \frac{\frac{\left(P_{f(plant)}\ x101325\right)\ Q_{f(plant)}\ )}{Q_{p(plant)}\ \varepsilon pump}+\frac{\left(\left(P_{f(Bp)}x101325\right)\right)Q_{f(Bp)}\ )}{Q_{p(plant)}\ \varepsilon_{Bp}}-\frac{(P_{f(in\ ERD)}\ x101325)\ Q_{f(ERD)}\ \varepsilon_{ERD}}{Q_{p(plant)}}}{36x10^5}$$

(36)

$P_{f(in\ ERD)}$ and $Q_{f(ERD)}$ are the retentate pressure and flow rate of stage 2 (Fig. 1).

The non-linear algebraic process model and the cost model equations can be written in a compact form as follows:

$$f(x, u, v) = 0 \qquad (37)$$

x is the set of all algebraic variables, u is the set of decision variables (to be optimised) and v denotes the constant parameters of the process. The function f is assumed to be continuously differentiable with respect to all their arguments. The model equations are solved using the gPROMS software, Model Builder 4.0 (Process System Enterprise Ltd., 2001).

3. Model validation

The process model presented in Section 2 is validated against the experimental data of Sundaramoorthy *et al.* (2011) where chlorophenol removal from aqueous solutions was considered. Fig. 2 shows a very good match for chlorophenol rejection for both the model presented and experimental results.

4. Multi-stage RO process description

Fig 2 shows the schematic diagram of a 3-stage RO wastewater treatment configuration connected in series. The proposed system consists of eight blocks, where each block represents ten parallel pressure vessels, with each pressure vessel containing a single membrane module. Stages 1 and 3 have three parallel blocks compared to stage 2, which consists of two blocks only. The design of stage 2 is corresponding with the lower feed flow rate compared to stages 1 and 3. This is due to the amalgamation of permeate streams of stage 1. However, stage 2 is working in line with the operation limits. The individual membrane element used is the spiral wound module of 7.8456 m² (Ion Exchange, India Ltd.) made of TFC Polyamide and suitable for low-pressure applications. This is the same as the one used by Sundaramoorthy *et al.* (2011) for the removal of chlorophenol from wastewater. The total membrane area of the 3-stage RO process is 627.65 m². Membrane specifications, including the transport parameters of water A_w and chlorophenol B_s, and the friction parameter b as used by Sundaramoorthy *et al.* (2011), are given for completeness in Table 1. A clear distinction with the study of Sundaramoorthy *et al.* (2011) is the fact that temperature dependent transport parameters are used, and these are given in Eqs. (14) and (15).

The proposed configuration is based on the combination of the retentate and permeate reprocessing design. The retentate from stage 1 is fed to stage 2 for further processing. The permeates from the stages 1 and 2 are mixed together and pressurised via the ERD and the booster pump before being fed to stage 3 for further processing. The high-pressure retentate from

the stage 2 transfers the energy to the low-pressure feed of stage 3. Stages 1 and 3 work at the same operating plant pressure value, which is at the maximum value of 24.77 atm. After the ERD, a booster pump is used to raise feed pressure at stage 3 to its desired value. Note, the proposed RO configuration is based on many sweater RO desalination plants for the Gulf region (Greenlee et al., 2013) but has not been considered for wastewater treatment.

Table 1. Membrane characteristics, design data and cost parameters

Parameter	Value
Supplier	Ion Exchange, India Ltd.
$A_{w(T_o)}$ and $B_{s(T_o)}$	$9.5188\text{x}10^{-7}\left(\frac{\text{m}}{\text{atm s}}\right)$ and $8.468\text{x}10^{-8}\left(\frac{\text{m}}{\text{s}}\right)$
T_o	31 (°C) (Experiment of Sundaramoorthy *et al.*, 2011)
Membrane friction factor (b)	$8529.45\left(\frac{\text{atm s}}{\text{m}^4}\right)$
Individual effective membrane area (A)	7.8456 (m^2)
Total membrane area of the plant	627.648 (m^2)
Height of the feed (t_f) and permeate (t_p) channels	0.0008 m and 0.0005 m
Effective membrane length (L) and width (W)	0.934 (m) and 8.4 (m)
Maximum feed pressure ($P_{f(in)}$) and temperature	24.77 (atm) and 40 °C
Minimum and maximum feed flow rate	$1\text{x}10^{-3}$ (m^3/s) and $1\text{x}10^{-4}$ (m^3/s)
High-pressure (ε_{pump}) and booster (ε_{Bp}) pumps efficiency	0.85 (-) and 0.85 (-)
ERD efficiency (ε_{ERD})	0.8 (-)
Motor efficiency (ε_{motor})	0.98 (-)
The discount rate (i)	8% (-)
The plant life (n)	25 (year)
Plant load factor (L_f)	0.85 (-)
The electricity unit cost (E_c)	0.08 ($/kWh)
The membrane element cost (C_{ele})	150 ($) *
The pressure vessel cost (C_{PV})	70 ($) *
The chemical treatment cost (C_{ct})	0.081 ($/$m^3$)
The cartridge filters replacement (C_{cf})	0.033 ($/$m^3$)

* : Email contact with the supplier (Ion Exchange, India Ltd.)

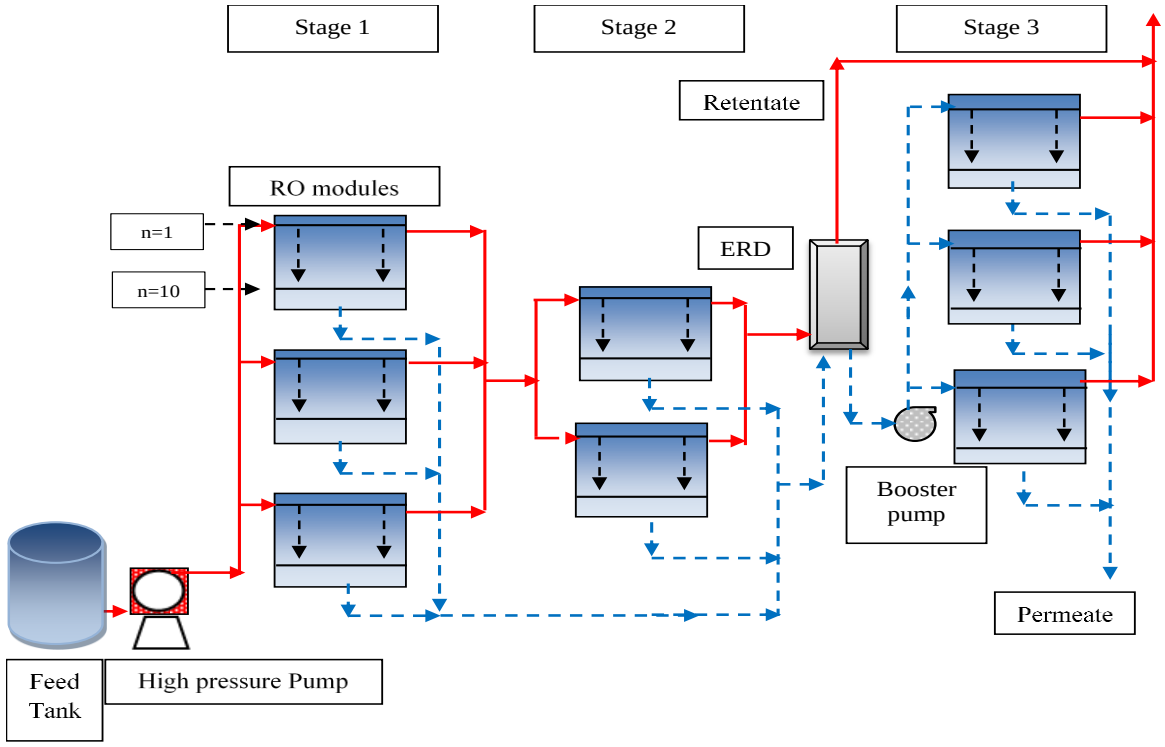

Fig. 1. Schematic diagram of the proposed RO process

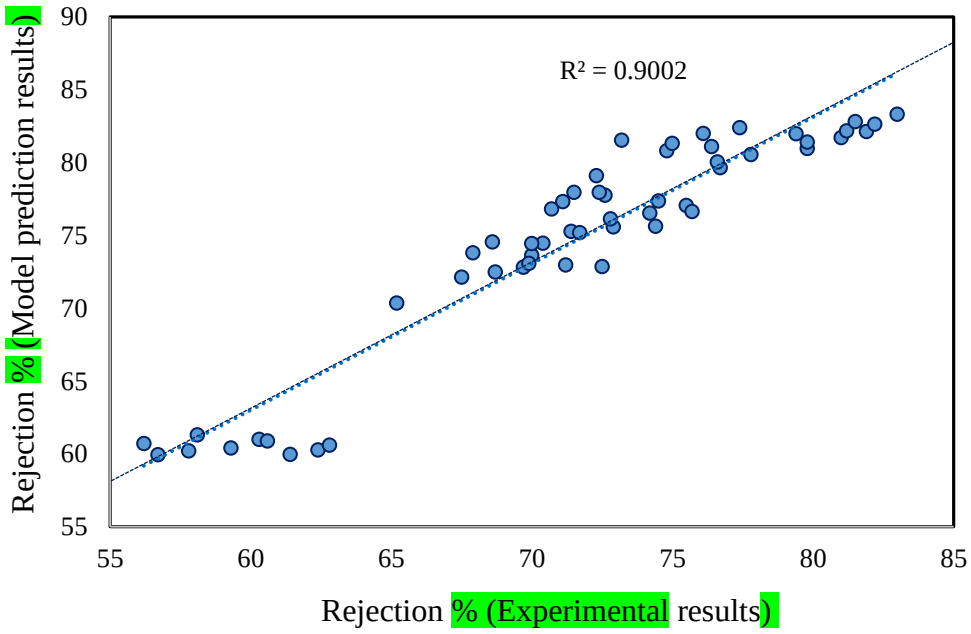

Fig.2. Model and experimental prediction results of chlorophenol rejection

5. Sensitivity analysis of operating conditions

The sensitivity analysis for the proposed model is carried out on the configuration shown in Fig. 1 (80 membrane elements, 1 membrane for each pressure vessel, and 10 membranes in each block) to assess the impact of the operating parameters; including the operating pressure, feed flow rate, concentration, and temperature on the process performance indicators. These are the chlorophenol rejection, the total recovery rate, the specific energy consumption as well as the total annualised cost and product unit cost. The impact of any selected parameter on the process performance is carried out by varying one parameter at a time while the other parameters remain fixed.

5.1 Impact of the feed pressure

Fig. 3 shows the simulation results of the total chlorophenol rejection $Rej_{(plant)}$ and total specific energy consumption SEC at various feed pressures. Also, Fig. 4 show the relation between the total annualized cost TAC and water product cost PUC with operating pressure variation. This simulation is carried out at fixed feed flow rate, concentration, and temperature of 0.006 m³/s, 0.006226 kmol/m³ (800.66 ppm) and 33 °C, respectively.

Fig. 3 shows that the operating pressure has inconsiderable impact on the chlorophenol rejection where it relatively fixed at 93%. This can be attributed to increasing water flux as a response to increasing pressure, which in turn increases the osmotic pressure and solute flux. In this respect, the simulation results confirmed that the considered variation of 69% in operating pressure at fixed other parameters causes a significant increase in the water recovery rate $Rec_{(plant)}$ of about 70.76%. However, a continuous increase in energy consumption is noticed as a response to increasing operating pressure (Fig. 3) despite the increase of recovery rate. It is fair to say that the fulfilling of high recovery rate necessitates high energy consumption to operate the pumps at high operating pressures (Fig. 3). However, the existence of ERD has a positive impact on reducing the energy required to operate the auxiliary booster pump.

The simulation results of Fig. 4 show that the total annualised cost TAC increases as the operating pressure increases. Specifically, increasing the operating pressure from 13 to 22 atm, with all other operating parameters fixed, the total annualised cost increases by around 23%; from 32610.46 to 40118.65 $/year. This can be explained by the corresponding increase of the total operating cost TOC of around 53.57% and the less significant increase of the total capital

cost TCC of 1.15%. Having said this, Fig. 4 shows a reduction of product unit cost PUC by around 13.62%. This reduction is attributed to a significant increase in the total product flow rate $Q_{p(plant)}$ of around 70.76% as a response to the operating pressure increase (noticed in the simulation results). It can therefore be said that the product unit cost decreases as a result to an increase in the demand of high-water recovery. This same point has already been confirmed by Coˆté *et al.* (2005) where the plant design of higher water flux caused by high pressure has resulted in lower costs. Fig. 4 shows that at high operating pressure beyond 18 atm (around 55% recovery rate), the total product cost is reduced only slightly.

The proposed design of this study (Fig. 1) has constrained the operation of stages 1 and 3 at a similar operating pressure, but one that requires a high amount of energy despite the increase of total product flow rate. Additionally, there is a further reduction of energy recovered by the ERD. This is caused by a continuous reduction of the retentate flow rate entering the ERD due to the increase in the operating pressure (Eq. 36). It is therefore not surprising to see a linear relationship between the operating pressure and specific energy consumption (Fig. 3).

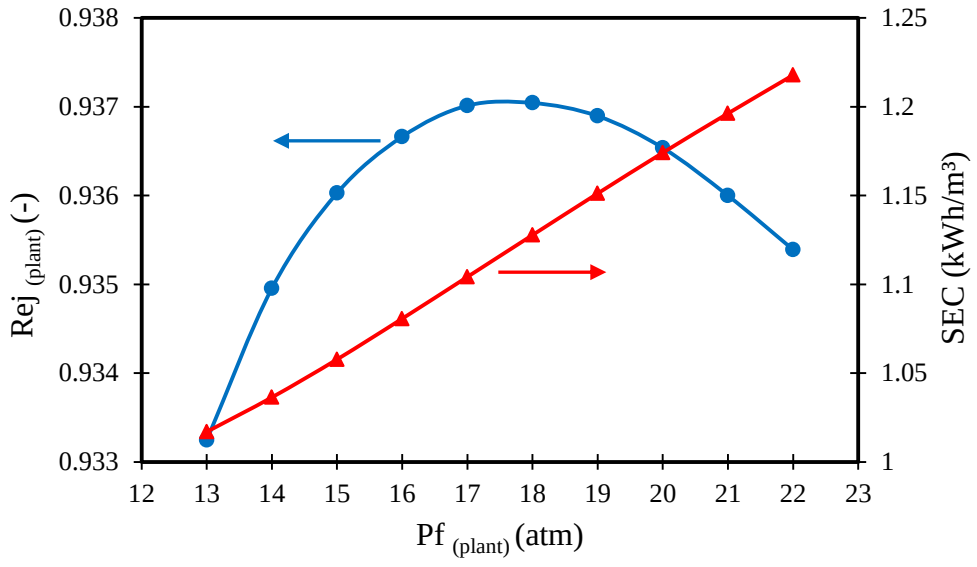

Fig. 3. The chlorophenol rejection and specific energy consumption versus the operating pressure (operating conditions: 0.006226 kmol/m³, 0.006 m³/s and 33 °C)

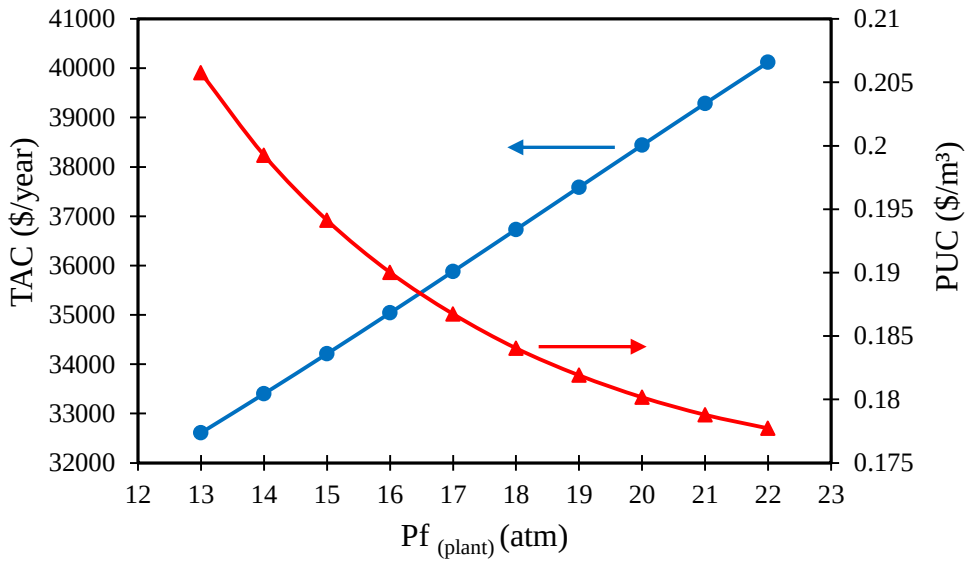

Fig. 4. The total annualised cost and water product unit cost versus the operating pressure (operating conditions: 0.006226 kmol/m³, 0.006 m³/s and 33 °C)

5.2 Impact of the feed flow rate

Figs. 5 and 6 show the simulation results of the chlorophenol rejection $Rej_{(plant)}$, specific energy consumption SEC, total annualised cost TAC, and product unit cost PUC, respectively, against the feed flow rate variation at fixed operating pressure, concentration, and temperature of 15 atm, 0.006226 kmol/m³ and 33 °C, respectively.

Fig. 5 depicts only 2.5% enhancement in chlorophenol rejecting due to increasing feed flow rate for the range of 0.0045 m³/s to 0.014 m³/s at constant other control variables. This is ascribed to reducing the concentration polarisation inside the modules due to increasing the fluid velocity. This in turn will reduce the accumulation of solute on the membrane surface and consequently reduces the solute flux. Moreover, it is concluded that increasing feed flow rate within the selected range would cause a considerable reduction of 65.4% in total water recovery $Rec_{(plant)}$, despite the improvement of around 7.6% carried out in total product flow rate $Q_{p(plant)}$. This is because the lower improvement of permeate flow rate against the increase in inlet feed flow rate. This is already pictured in Eq. (9).

In addition, Fig. 5 depicts a significant increase in the specific energy consumption of around 146.4% due to an increase in the feed flow rate. This is occurred despite the improvement of product flow rate $Q_{p(plant)}$ of around 7.61%. Basically, the energy consumption is controlled by

the variation of flow rate and operating pressure as demonstrated in Eq. (36). Therefore, it is fair to say that any optimisation of the energy consumption requires a bit modification on pressure and flow rate.

Fig. 6 shows a clear increase of around 113.9% and 84.78.1% in the total annualised cost TAC and product unit cost PUC, respectively, as a direct result of the feed flow rate variation from 0.0045 m³/s to 0.014 m³/s. The cause for this is the significant increase in the total capital cost TCC and operating cost TOC of around 129.8% and 95.47%, respectively. This significant increase is due to the increase of the wastewater intake and pre-treatment cost, the capital cost of high-pressure pump and the capital cost of ERD, which are function of plant feed flow rate. Moreover, the increase of the product unit cost PUC is due to lower product flow rate caused by an increasing feed flow rate. These results are interesting in that they show an insignificant impact (of around 1.15%) of the operating pressure on the total capital cost TCC. One conclusion that can be made is that the product unit cost is progressively increased with the feed flow rate compared to pressure.

To summarise, the above two simulation results of feed pressure and flow rate have revealed that both the total annualised cost TAC and product unit cost PUC are sensitive to the operating pressure and feed flow rate. Increasing the feed flow rate at fixed operating pressure causes higher demand of total annualised cost (113.9%) in comparison to (23%) after increasing the operating pressure at fixed feed flow rate. The unit product cost is improved after increasing the operating pressure at constant feed flow rate by 13.62%, whilst there is a significant increase of 84.78.1% in case of feed flow rate variation at constant operating pressure. Both simulations have been carried out at fixed operating concentration and temperature. Additionally, increasing the feed flow rate at constant pressure has a considerable bad impact on the specific energy consumption compared to the operating pressure at fixed feed flow rate.

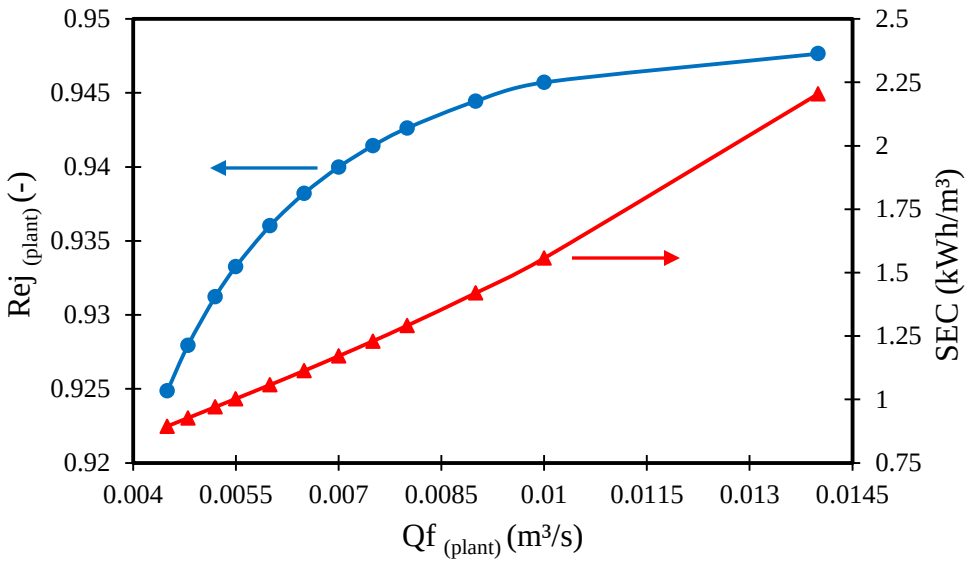

Fig. 5. The chlorophenol rejection and specific energy consumption versus the operating feed flow rate (operating conditions: 0.006226 kmol/m³, 15 atm and 33 °C)

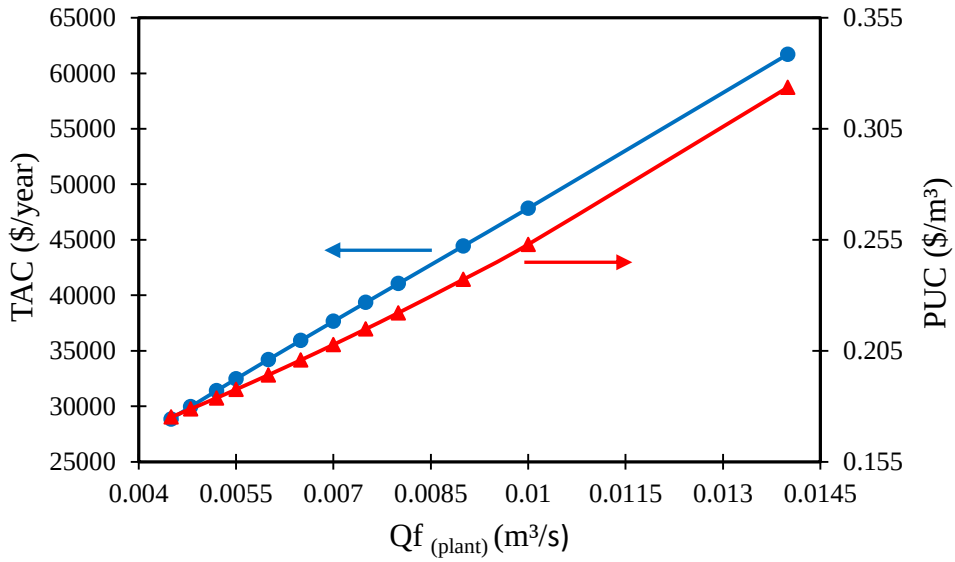

Fig. 6. The total annualised cost and water product unit cost versus the operating feed flow rate (operating conditions: 0.006226 kmol/m³, 15 atm and 33 °C)

5.3 Impact of the feed concentration

Figs. 7 and 8 present the response in the chlorophenol rejection $Rej_{(plant)}$, specific energy consumption SEC, total annualised cost TAC, and product unit cost PUC, respectively, for the variation of feed concentration from 0.000778 kmol/m³ to 0.012 kmol/m³ at fixed operating pressure, flow rate, and temperature of 15 atm, 0.006 m³/s and 33 °C, respectively.

Fig. 7 shows a significant increase of rejection parameter at low feed concentrations corresponding with a slow increase at high operating concentrations. In overall, the simulation showed an increase of 20% in chlorophenol rejection due to concentration variation. This phenomenon can be ascribed to increasing the solute flux at high feed concentration, which mitigates the progress of chlorophenol rejection. Al-Obaidi and Mujtaba (2016) confirmed the improvement of membrane strength to remove pollutants as a result to increasing feed concentration. However, this is not the case of high concentration solutions such as seawater. In the same aspect, a decrease of around 16.2% is occurred in the recovery rate as a response to concentration variation. Broadly speaking, increasing feed concentration causes a reduction in water flux due to increasing the osmotic pressure.

Fig. 7 shows the attaining of a minimum specific energy consumption at an optimum feed concentration (between 0.003891 and 0.006226 kmol/m³). However, it is easy to see the variation of the energy consumption, which can be ascribed to the consumed power of pumps and gained power of ERD, as demonstrated in Eq. 36. Specifically, increasing the feed concentration up to 0.006226 kmol/m³ at fixed other operating conditions showed a regular reduction of energy consumption by around 2%. In this aspect, the simulation confirmed a noticeable increase in the retentate flow rate of stage 2 (the feed stream of ERD) that corresponding to a high impact of ERD in reducing the total energy consumption of the plant. Occasionally, this is equivalent to a continuous reduction of total product flow rate of stage 2 entering the booster pump. However, the simulation confirmed a lower efficiency of ERD to reduce the total energy consumption due to insignificant increase of the retentate flow rate of stage 2 entering the ERD after increasing the feed concentration from 0.006226 kmol/m³ to 0.012 kmol/m³. This in turn causes a clear increase of energy consumption after 0.006226 kmol/m³ of feed concentration and a minimum value to be existed in the specific energy consumption due to the variation of feed concentration. Moreover, it is important to mention that

increasing the feed concentration causes an increase in the pressure loss inside all the membranes that corresponding to decrease the retentate pressure of stage 2 entering the ERD.

Fig. 8 shows that feed concentration variation has an advantage of a slight decrease of the total annualised cost TAC around 4.61% despite the reduction of water recovery rate. Interestingly, the lowering of the total annualised cost has not materialised for the other operating tested parameters of feed pressure, flow rate, and temperature. This phenomenon is attributed to the reduction of total operating cost TOC and total capital cost TCC around 9.99% and 0.05%, respectively, which occurred as a result to increasing the operating concentration.

The simulation results clearly confirm a reduced annual spare cost of around 16.23%, annual labor cost of around 16.23%, maintenance cost of around 9% and brine disposal cost of around 16.23%. All these costs are dependent on the total product flow rate $Q_{p(plant)}$, which is decreased as a result of an increase in the operating concentration. Fig. 8 shows that the product unit cost PUC increases by around 8.61% due to an increase of the operating concentration for the same above reason.

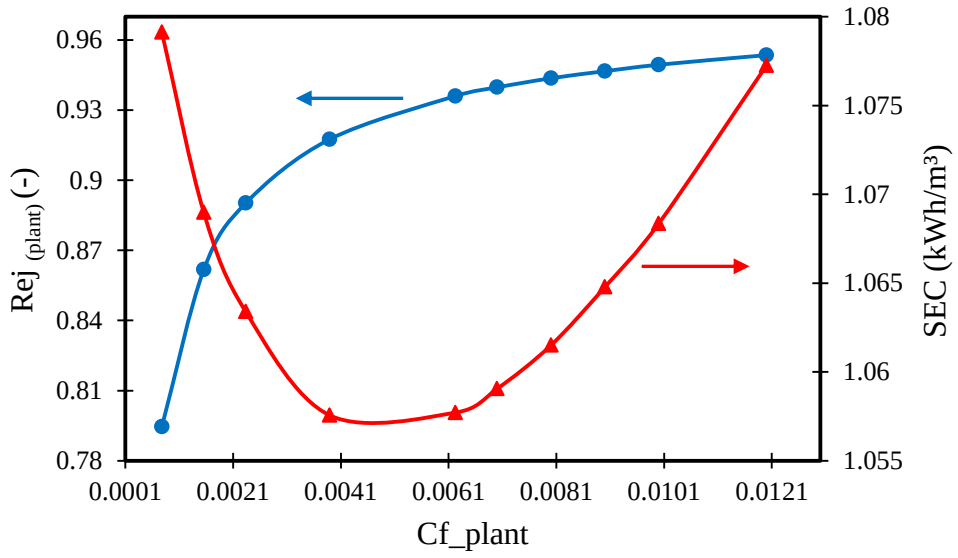

Fig. 7. The chlorophenol rejection and specific energy consumption versus the operating concentration (operating conditions: 15 atm, 0.006 m³/s and 33 °C)

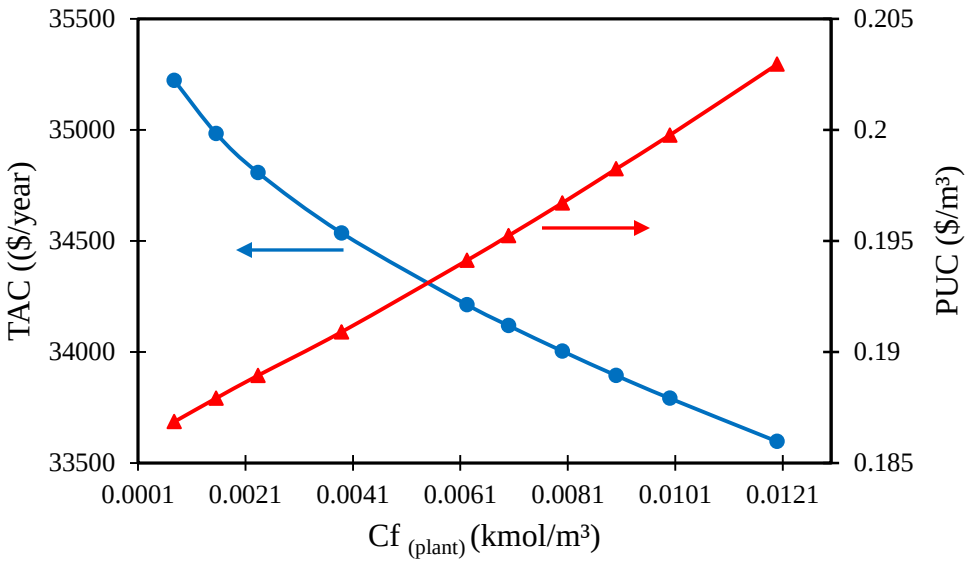

Fig. 8. The total annualised cost and water product unit cost versus the operating concentration (operating conditions: 15 atm, 0.006 m³/s and 33 °C)

5.4 Impact of the feed temperature

The impact of the operating temperature variation between 30 °C and 40 °C (by 33%) on the chlorophenol rejection $Rej_{(plant)}$, specific energy consumption SEC, total annualised cost TAC and product unit cost PUC, is plotted in Figs. 9 and 10, respectively, at fixed feed pressure, concentration and flow rate of 15 atm, 0.006226 kmol/m³ and 0.006 m³/s, respectively.

Fig. 9 confirms that increasing the temperature has a noticeable effect of around 9.7% on the chlorophenol rejection. Basically, increasing the fluid temperature aids to reduce its viscosity and density, which in turn increases the water flux. In this respect, the recovery rate increases by around 37.7% as a response to the temperature. This is also obtained by Madaeni *et al.* (2006).

Fig. 9 shows the reduction of specific energy consumption by around 13.7% as the exceptional specification of feed temperature compared to other tested cooperating conditions, which confirmed an increase of energy consumption (Figs. 3, 5 and 7). The increase of permeate flow rate due to increasing temperature would explain the reduction of energy consumption.

It also appears that the demand of total annualised cost TAC increases by around 6.93% (Fig. 10) as a response to the operating temperature variation compared to 23% and 113.9% for the tested variations of feed pressure (Fig. 4) and feed flow rate (Fig. 6), respectively. The increase of TAC as a result to increasing feed temperature is ascribed to a corresponding increase in the total

capital cost (TCC) and the total operational cost (TOC). Specifically, TCC increases due to increasing the capital cost of high-pressure pump and booster pump C_{Pump} as denoted in Eq. 20 as a result of improving the feed flow rate of stage 3. Also, TOC increases with increasing temperature due to increasing pumping operating cost OC_{Pu}, net pumping cost OC_{np}, annual operating spares cost OC_{sc}, effluents disposal cost OC_{bd}, annual labour cost OC_{lab}, and annual maintenance cost OC_{main}, as a result to improving the plant permeate flow rate (see Eqs. 23, 25, 28, 30, 32, and 35, respectively). A key aspect of the operating temperature increase is the reduction of product unit cost PUC by about 17% (Figs. 10), which is caused by an increase of 37.7% in total product flow rate $Q_{p(plant)}$. This can be compared to a reduction in product unit cost PUC of around 13.62% as a response to the operating pressure variation from 13 atm to 22 atm at fixed other operating parameters (Fig. 4).

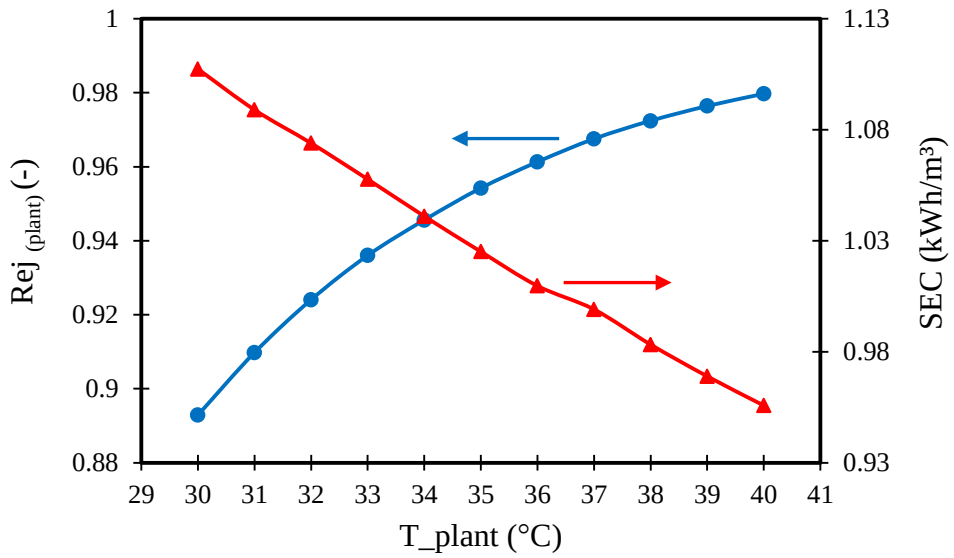

Fig. 9. The chlorophenol rejection and specific energy consumption versus the operating feed temperature (operating conditions: 0.006226 kmol/m³, 15 atm and 0.006 m³/s)

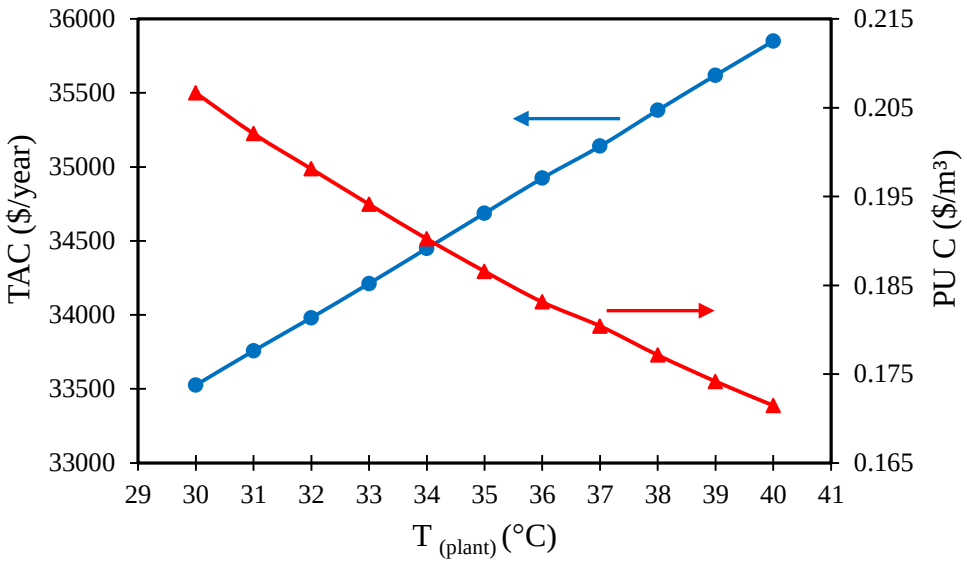

Fig. 10. The total annualised cost and product unit cost versus the operating feed temperature (operating conditions: 0.006226 kmol/m³, 15 atm and 0.006 m³/s)

To summarise the simulation results of the above section, it can be said that the sensitivity analysis is carried out by investigating the impact of several operating conditions of the proposed multi-stage RO plant on the performance indicators and economic parameters. The following observations are affirmed:

- The chlorophenol rejection is highly and positively affected by the increase of operating temperature. Therefore, it might be adequate to achieve the chlorophenol treatment at high temperature. Preheating the feed would be an efficient option despite the possibility of increasing the treatment cost.
- The recovery rate is highly affected by the increase of operating pressure. However, the feed flow rate and concentration increase are negatively affected the recovery rate.
- The specific energy consumption is positively affected by the increase of temperature compared to the other operating conditions. However, an optimum feed concentration can attain the lowest energy consumption.
- Increasing the operating temperature or pressure can reduce the product unit cost with significant positive impact for temperature. This is compared to the impact of increasing the operating concentration or feed flow rate with significant passive impact for operating flow rate.

- The total annualised cost increases as a result to an increase in the operating pressure, flow rate and temperature, but the operating temperature has the lowest impact. However, a slight reduction in the total annualised cost is noticed due to increasing the operating concentration.
- Increasing the operating concentration while keeping other operating parameters constant yields reduced annual spare cost, labor cost, maintenance cost and brine disposal cost.

Simulation results of the multi-stage RO configuration shown in Fig. 1, are given in Table 2 for the following set of operating conditions: 0.006226 kmol/m³, 0.009 m³/s (777.6 m³/day), 15 atm and 32 °C of feed concentration, flow rate, pressure, and temperature, respectively.

Table 2 shows the performance of the proposed plant with the estimation of all the economic terms of this process including the capital and operating costs. It can be readily noticed that the total product unit cost of this plant is 0.242 ($/m³) with total energy consumption of 1.443 (kWh/m³). These costs can be optimised further for larger plant sizes.

For a better evaluation of the variability between the cost parameters, Fig. 11 shows the contribution of the cost parameters on the total annualised cost of the proposed plant measured by the relative ratio of each parameter to the total annualised cost. It is evident from Fig. 11 that the contribution of the cost elements to the total annualised cost can be varied. Specifically, the annual operating net pumping cost OC_{np} represents the biggest contribution on the total annualised cost (compared to other operating cost parameters). This is consistent with the case of seawater desalination, which shows the same findings. Patroklou and Mujtaba (2014) confirmed that the operating pumping cost (only high-pressure pump) has the highest contribution to the total annualised cost of a medium-size RO desalination plant of 68 parallel pressure vessels (one membrane per each pressure vessel), albeit with the constraint of this model not having considered labor cost calculations.

Table 2. Simulation results of the proposed multi-stage RO plants (Fig. 1)

$Cp_{(plant)}$ (kmol/m³)	$Qp_{(plant)}$ (m³/s), (m³/day)	$Qr_{(plant)}$ (m³/s)	$Rej_{(plant)}$ (-)	$Rec_{(plant)}$ (-)	C_{wwip} ($)	C_{Pump} ($)	C_{ERD} ($)	C_{me} ($)	TCC ($)	
4.117×10^{-4}	2.752×10^{-3} 237.77	6.247×10^{-3}	0.933	0.305	204580.55	2602.61	2191.09	17600.0	25620.85	
OC_{np} ($/year)	OC_{sc} ($/year)	OC_{ch} ($/year)	OC_{lab} ($/year)	OC_{me} ($/year)	OC_{maint} ($/year)	OC_{bd} ($/year)	TOC ($/year)	TAC ($)	PUC ($/m³)	SEC (kWh/m³)
7155.09	2434.82	4342.50	1736.06	2400.0	420.38	130.20	18619.07	44239.93	0.242	1.443

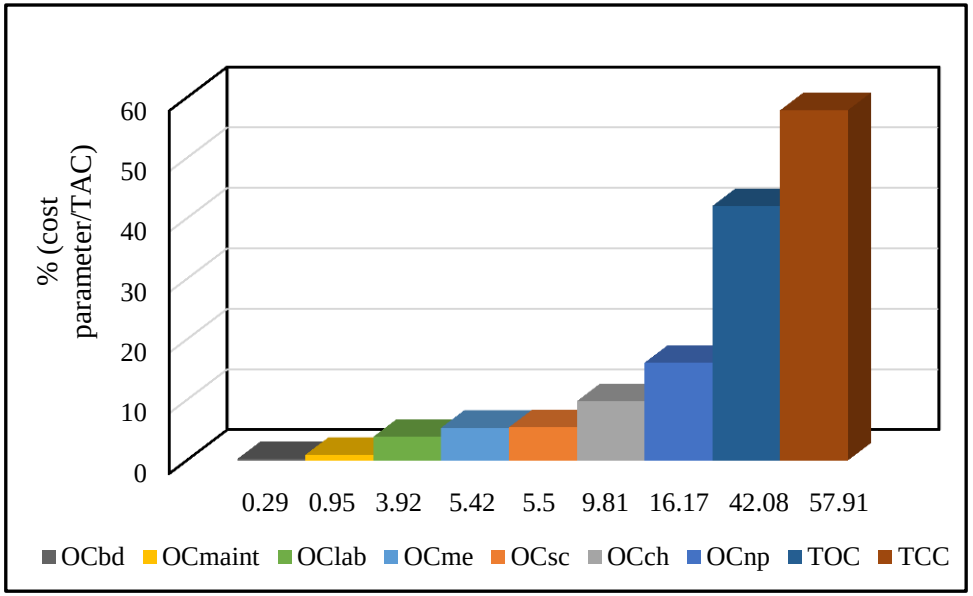

Fig. 11. Cost elements contribution on total annualised cost of the proposed plant

The simulation results and the calculations of cost parameters provide a detailed picture of the product unit costs and specific energy consumption costs of the proposed RO plants. However, the authors believe that there is a possibility for reducing these costs further and at the same time achieving a higher recovery and chlorophenol rejection rates. To achieve this, a multi-objective optimisation methodology is developed as discussed in the next section.

6. Multi-objective optimisation methodology

This section attempts to optimise the product unit cost of treated water in combination with the total annualised cost and energy consumption at high quality wastewater using the proposed configurations of the RO wastewater treatment shown in Fig. 1.

The optimisation methodology includes the following criteria:

- The optimisation of the treatment process is restricted to a realistic recovery rate of at least 50%.
- A maximum operating pressure of 24.77 atm is selected as it represents the maximum pressure that the membrane module Ion Exchange, India Ltd. (7.8456 m^2) can hold.
- The restricted manufacture lower and upper limits of operating flow rate for any membrane in the system are selected as $1x10^{-4}$ m^3/s to $1x10^{-3}$ m^3/s.
- The minimum value of 90% is selected as the chlorophenol rejection to maintain the process with high quality product.
- The minimum operating temperature of 30 °C is selected to corresponding the mass transfer model Eq. (1) and the model transport parameters, which are based on the experimental work of Sundaramoorthy *et al.* (2011).
- Three upper limits of operating temperature will be selected as 30 °C, 35 °C and 40 °C to handle different industrial effluents.

It is noteworthy to mention that the optimisation problem has three optimisation sub-problems in line with the three industrial effluents temperatures selected.

The non-linear optimisation method used to optimise the operation of wastewater treatment system considering the chlorophenol removal using the retentate-permeate reprocessing design of multi-stage RO process is described below

Given:

- Feed chlorophenol concentration, feed temperature (30 °C or 35 °C or 40 °C), module specifications, membrane elements and pressure vessels number

Determine:

- Optimal feed pressure and feed flow rate (continuous variables)

So as to:

- Minimise: The product unit cost
- Minimise: The total annualised cost
- Minimise: The specific energy consumption

Subject to:

- Equality (process model) and inequality constraints including the operational parameters of the plant and each membrane element (linear bounds of optimisation variables).

The optimisation problem can therefore be written mathematically as follows:

$$\begin{array}{ll} \text{Min} & PUC \\ \text{Min} & TAC \\ \text{Min} & SEC \\ P_{f(plant)}, Q_{f(plant)} & \end{array}$$

Subject to:

Equality constraints:

Process Model: $f(x, u, v) = 0$

Inequality constraints:

$$(10\ \text{atm}) \quad P_{f(plant)}{}^{L} \leq P_{f(plant)} \leq P_{f(plant)}{}^{U} \quad (24.771\ \text{atm})$$

$$(3\text{x}10^{-3}\ \text{m}^3/\text{s}) \quad Q_{f(plant)}{}^{L} \leq Q_{f(plant)} \leq Q_{f(plant)}{}^{U} \quad (3\text{x}10^{-2}\ \text{m}^3/\text{s})$$

End-point constrains: $Rec_{(plant)} \geq 50\%$

$$Rej_{(plant)} \geq 90\%$$

$$T_{(plant)} = 1))\ 30\ °\text{C}, \quad 2))\ 35\ °\text{C}, \quad 3))\ 40\ °\text{C}$$

$$(1\text{x}10^{-4}\ \text{m}^3/\text{s}) \quad Q_{f(membrane)}{}^{L} \leq Q_{f(membrane)} \leq Q_{f(membrane)}{}^{U} \quad (1\text{x}10^{-3}\ \text{m}^3/\text{s})$$

L and U are the lower and upper limits, respectively. The optimisation problem was solved by the Successive Quadratic Programming SQP method using the gPROMS software suite.

The Successive Quadratic Programming (SQP) method is already included in the gPROMS software suits and used to solve steady state optimisation problems by implementing a first-order Taylor's series approximation around as initial point specified in the process. This in turn will convert the nonlinear functions into approximate linear functions. In other words, the process started by converging all the equality constraints (including the model equations in its compact form) and specified the inequality constraints. Secondly, the optimisation step started by updating (reinitialization) the values of decision variables (Edgar et al. 2001). Specifically, reinitialization of the decision locates a new search direction for the decision

variables, which is achieved using the solution of the last successful iteration. The new values of the decision variables will be the initial point (guestimate values) for further linearization to solve the linear problem. This is continued until solving the linear problem with a specific improvement of the objective functions. It is noteworthy to mention that one of the standard solvers in gPROMS software for optimisation problems is CVP_SS, which employs the DASOLV code. This solver is quite able to solve steady state and dynamic optimisation problems with both discrete and continuous optimisation decision variables (mixed integer optimisation).

6.1 Optimisation results and discussion

Table 3 shows the optimised results of the proposed plant considering the removal of chlorophenol from wastewater. The results include the optimum product unit cost, total annualised cost, specific energy consumption, chlorophenol rejection, total water recovery and the operation feed flow rate and pressure at three operating temperatures and fixed feed concentration of 0.006226 kmol/m³.

Table 3. Optimisation results of the proposed plant at operating concentration of 0.006226 kmol/m³

$T_{(plant)}$, (°C)	$Q_{f(plant)}$, (m³/s) (m³/day)	$P_{f(plant)}$, (atm)	PUC, ($/m³)	TAC, ($/year)	SEC, (kWh/m³)	$Q_{p(plant)}$, (m³/s) (m³/day)	$Rej_{(plant)}$ (-)	$Rec_{(plant)}$ (-)
30	$6.771\text{x}10^{-3}$ 585.01	19.916	0.199	40236.06	1.309	$3.386\text{x}10^{-3}$ 292.57	0.900	0.500
35	$4.303\text{x}10^{-3}$ 371.77	13.002	0.173	27116.75	0.799	$2.463\text{x}10^{-3}$ 212.79	0.943	0.572
40	$4.037\text{x}10^{-3}$ 348.79	10.798	0.167	25363.89	0.669	$2.346\text{x}10^{-3}$ 202.68	0.970	0.581

Table 3 clearly shows the importance of the operating temperature in the treatment process where the restriction of the optimisation methodology with 30 °C has an impact on the operating feed flow rate and pressure in order to guarantee the minimum value of rejection $Rej_{(plant)}$ of 90%. Table 3 also shows that the optimisation has reduced the product unit cost and total annualised cost compared to the simulation results of Table 2. It is interesting to see that running the process at 35 °C actually enhances both the rejection and total recovery rate. This is corresponding with reducing the specific energy consumption SEC as a result of increasing the total product flow rate. More importantly, the optimisation has been implemented to minimise the specific energy consumption (as an objective function). The methodology used readily selected lower operating pressures after increasing the operating

temperature to 35 °C and 40 °C. This accelerate the water flux and enhance the chlorophenol rejection, and therefore yields reduced product unit cost by around 7.5% when the operating temperature increased from 30 °C to 40 °C.

The process treatment of the proposed plant has shown promising results in terms of increased rejection at high operating temperatures. This result has therefore motivated the authors to find a way to estimate the maximum chlorophenol rejection that can be achieved, and this is discussed in the next section.

In this particular case, the approximated cost of 90 – 97% chlorophenol removal is around 0.167 – 0.199 $/m³ for the RO plant capacity of 202.68 – 292.57 m³/day. It is clear that the RO treatment cost of the secondary industrial effluents is always less than the seawater desalination cost. This is due to the use of low operating pressure, low operating concentration with high recovery rate in the RO wastewater process compared to seawater desalination process.

6.2 Optimum operating conditions with higher chlorophenol rejection

The efficiency of any wastewater treatment plant is measured by the capacity of removing the pollutants from secondary industrial effluents. The aim of this section is to investigate the operational conditions of the proposed plant shown in Fig. 1 that will yield the maximum chlorophenol rejection and yet at operating concentration of 0.006226 kmol/m³ and one that can achieve at least 50% total water recovery.

The above can be written mathematically as follows for the corresponding non-linear optimisation problem:

$$\underset{P_{f(plant)}, Q_{f(plant)}, T_{(plant)}}{\text{Min}} \quad Rej_{(plant)}$$

Subject to:

- Equality constraints:

Process Model: $f(x, u, v) = 0$

- Inequality constraints:

$$(10 \text{ atm}) \quad P_{f(plant)}{}^{L} \leq P_{f(plant)} \leq P_{f(plant)}{}^{U} \quad (24.771 \text{ atm})$$

$$(3\text{x}10^{-3} \text{ m}^3\text{/s}) \quad Q_{f(plant)}{}^{L} \leq Q_{f(plant)} \leq Q_{f(plant)}{}^{U} \quad (3\text{x}10^{-2} \text{ m}^3\text{/s})$$

$$(30 \text{ °C}) \quad T_{(plant)}{}^{L} \leq T_{(plant)} \leq T_{(plant)}{}^{U} \quad (40 \text{ °C})$$

End-point constrain: $Rec_{(plant)} \geq 50\%$

$$(1\text{x}10^{-4} \text{ m}^3\text{/s}) \quad Q_{f(membrane)}{}^{L} \leq Q_{f(membrane)} \leq Q_{f(membrane)}{}^{U} \quad (1\text{x}10^{-3} \text{ m}^3\text{/s})$$

Table 4 shows that a maximum chlorophenol rejection of 98.8% can be achieved at maximum operating pressure and temperature. However, the increased chlorophenol rejection comes at an increased total annualised cost compared to that of case 3 as shown in Table 3. In fact, the chlorophenol rejection can be increased further when using other membranes which can operate at higher operating pressure.

Table 4. Optimum operating condition of maximum chlorophenol rejection at feed concentration of 0.006226 kmol/m³

$Q_{f(plant)}$, (m³/s) (m³/day)	$P_{f(plant)}$, (atm)	$T_{(plant)}$, (°C)	$Rej_{(plant)}$ (-)	$Rec_{(plant)}$ (-)	$Q_{p(plant)}$, (m³/s) (m³/day)	PUC, ($/m³)	TAC, ($/year)	SEC, (kWh/m³)
1.198×10^{-2} 1034.98	24.771	40	0.988	0.500	5.987×10^{-3} 517.27	0.210	68882.73	1.767

7. Conclusions

In this paper, a set of mathematical model equations for the spiral-wound RO process based on the removal of chlorophenol from wastewater has been developed. Firstly, the model is validated against experimental data of chlorophenol removal from the literature and was accurate enough to predict the process performance according to a wide range of operating parameters. Secondly, the validated model has been augmented with a detailed cost estimation model for removing chlorophenol from wastewater using a multi-stage RO plant.

This research has presented a new design of permeate reprocessing that yields a high removal of chlorophenol compared to other similar published attempts, with a detailed cost calculation and a sensitive analysis. Analysis results show that the operating pumping cost has the highest contribution to the total annualised cost of RO wastewater treatment. Moreover, a multi-objective optimisation is carried out to optimise the operation of wastewater treatment system considering the chlorophenol removal. In the light of the optimisation results obtained for the proposed RO plant of 80 membrane elements, it is possible to remove 90% – 97% of chlorophenol at an estimated unit product cost of 0.199 – 0.167 $/m³, approximated total annualised cost of 40236.06 – 25363.89 $/year, specific energy consumption of 1.309 – 0.669 kWh/m³ that adequates with a recovery rate of 50% – 58.1% at operating temperature between 30 °C and 40 °C. A further optimisation study was carried out to maximise the chlorophenol rejection, and this shows that 98.8% of chlorophenol can be removed at approximately 0.21 $/m³ of the production capacity of 517.27 m³/day RO plant. It is hoped that the research discussed in this paper goes a long way to reduce the knowledge gap in the

economic aspect of RO wastewater treatment process. This research also shows that there is a further possibility of lowering the product unit cost by implementing novel membranes with high water permeability using the technique of optimisation outlined in this paper. Finally, the work carried out in this research should prove useful for comparing different wastewater RO plants from an economic perspective.

Nomenclature

A : The effective area of the membrane (m^2)

$A_{w(T)}$: The solvent transport coefficient at any operating temperature (m/atm s)

$A_{w(T_o)}$: The solvent transport coefficient at reference temperature (m/atm s)

b : The feed channel friction parameter (atm s/m^4)

B_s : The solute transport coefficient (m/s)

$CCRF$: The capital cost recovery factor (dimensionless)

C_b : The bulk feed solute concentrations at the feed channel ($kmol/m^3$)

C_{chc} : The capital charge cost ($)

C_{cf} : The cost of cartridge filters replacement ($/m^3$)

C_{ct} : The chemical treatment cost per cubic meter of feed ($/m^3$)

C_{ele} : The membrane element cost ($)

C_f : The inlet feed solute concentrations at the feed channel ($kmol/m^3$)

C_{lab} : The labor cost ($/m^3$)

C_m : The dimensionless solute concentration in Eq. (5) in Table A.1 in Appendix A (dimensionless)

C_{main} : The maintenance cost ($/m^3$)

C_{me} : The membrane module and pressure vessel capital cost ($)

C_p : The permeate solute concentration at the permeate channel ($kmol/m^3$)

C_{PV} : The pressure vessel cost ($)

C_w : The solute concentration on the membrane surface at the feed channel ($kmol/m^3$)

C_{wwip} : The wastewater intake and pre-treatment cost ($)

C_{Pump} : The capital cost of high-pressure pump and booster pump ($)

C_{ERD} : The capital cost of energy recovery device ($)

D_b : The solute diffusion coefficient of feed at the feed channel (m^2/s)

D_p : The solute diffusion coefficient of feed at the permeate channel (m^2/s)

de_b : The equivalent diameters of the feed channel (m)

de_p : The equivalent diameters of the permeate channel (m)

E_c : The unit power cost (dimensionless)

E_{pump} : The energy consumption of high-pressure pump (kW h/m³)

E_{ERD} : The recovered energy of by turbine (kW h/m³)

i : The discount rate (dimensionless)

J_s : The solute molar flux through the membrane (kmol/m² s)

J_w : The permeate flux (m/s)

k : The mass transfer coefficient at the feed channel (m/s)

L : The membrane length (m)

L_f: The plant load factor per annum (dimensionless)

LPV : The length of pressure vessel (m)

m_f : Parameter in Eqs. (10) and (11) in and defined in Eq. (12) in Table A.1 in Appendix A

n : The plant life (year)

N_{ele} : Number of membrane elements per pressure vessel (dimensionless)

OC_{ERD} : The annual ERD operating cost ($/year)

OC_{ch} : The annual chemical treatment cost ($/year)

OC_{lab} : The annual labor operating cost ($/year)

OC_{maint} : The annual maintenance operating cost ($/year)

OC_{me} : The annual membrane replacement operating cost ($/year)

OC_{np} : The annual net operating pumping cost including the pumps and ERD ($/year)

OC_{Pu} : The annual net pumping cost ($/year)

OC_{sc} : The annual operating spares cost ($/year)

$P_{f(Bp)}$: Supplied pressure of the booster pump (atm)

$P_{f(in)}$: The inlet feed pressure (atm)

$P_{f(outERD)}$: The supplied pressure of energy recovery device (atm)

$P_{f(out_{stage})}$: The retentate pressure of a specified stage (atm)

$P_{f(out)}$: The outlet feed pressure (atm)

$P_{f(plant)}$: The operating plant pressure (atm)

P_p : The permeate channel pressure (atm)

PUC : The water product unit cost ($/m³)

Q_b : The bulk feed flow rate at the feed channel (m³/s)

Q_f : The inlet feed flow rate at the feed channel (m³/s)

$Q_{f(membrane)}$: The membrane feed flow rate (m³/s)

$Q_{f(plant)}$: The plant operating flow rate (m³/s)

Q_p : The permeate flow rate at the permeate channel (m³/s)

$Q_{p(plant)}$: The total plant product flow rate (m³/s)

Q_r : The retentate flow rate at the feed channel (m³/s)

R : The gas low constant (R=0.082 atm m³/ K kmol)

Re_f : The Reynold number at the feed channel (dimensionless)

Rec : Total water recovery of an individual membrane (dimensionless)

$Rec_{(plant)}$: The plant total water recovery (dimensionless)

Rej : The solute rejection coefficient of an individual membrane (dimensionless)

$Rej_{(plant)}$: The total plant chlorophenol rejection (dimensionless)

Re_p : The Reynold number at the permeate channel (dimensionless)

SEC : The specific energy consumption (kWh/m³)

T : The feed temperature (°C)

$T_{(plant)}$: The operating plant temperature (°C)

T_o : Reference temperature of Sundaramoorthy *et al.* (2011) experiments (°C)

TAC : Total annualised cost ($/year)

TCC : The total capital cost ($/year)

TOC : The total operating cost ($/year)

t_f : The height of the feed spacer (m)

t_p : The height of permeate channel (m)

U_b : The bulk feed velocity at the feed channel (m/s)

W : The membrane width (m)

Greek

μ_b : The Feed viscosity at the feed channel (kg/m s)

μ_p : The permeate viscosity at the permeate channel (kg/m s)

ρ_b : The feed density at the feed channel (kg/m³)

ρ_p : The permeate density at the permeate channel (kg/m³)

ρ_w : The molal density of water (55.56 kmol/m³)

θ : Parameter in Eq. (23) defined in Eq. (24) in Table A.1 in Appendix A

ε_{pump} : The pump efficiency (dimensionless)

ε_{Bp} : The booster pump efficiency (dimensionless)

ε_{motor} : The motor efficiency (dimensionless)

ε_{ERD} : The energy recovery device efficiency (dimensionless)

References

Amar N.B., Kechaou N., Palmeri J., Deratani A., Sghaier A., 2009. Comparison of tertiary treatment by nanofiltration and reverse osmosis for water reuse in denim textile industry. *Journal of Hazardous Materials*, 170(1) 111–117.

Al-Obaidani S., Curcio E., Macedonio F., Di Profio G., Al-Hinai H., Drioli E., 2008. Potential of membrane distillation in seawater desalination: Thermal efficiency, sensitivity study and cost estimation. *Journal of Membrane Science*, 323, 85-98.

Al-Obaidi M.A., Mujtaba I.M., 2016. Steady state and dynamic modelling of spiral wound wastewater reverse osmosis process. *Computers and Chemical Engineering*, 90, 278-299.

Al-Obaidi M.A., Kara-Zaïtri C., Mujtaba I.M., 2017a. Removal of phenol from wastewater using spiral-wound reverse osmosis process: Model development based on experiment and simulation. *Journal of Water Process Engineering*, 18, 20-28.

Al-Obaidi M.A., Li J.-P., Kara-Zaïtri C., Mujtaba I.M., 2017b. Optimisation of reverse osmosis based wastewater treatment system for the removal of chlorophenol using genetic algorithms. *Chemical Engineering Journal*, 316, 91-100.

Al-Obaidi M.A., Kara-Zaïtri C., Mujtaba I.M., 2018a. Simulation and optimisation of a two-stage/two pass reverse osmosis system for improved removal of chlorophenol from wastewater. *Journal of Water Process Engineering*, 22, 131-137.

Al-Obaidi M.A., Kara-Zaïtri C., Mujtaba I.M., 2018b. Performance evaluation of multi-stage and multi-pass reverse osmosis networks for the removal of N-nitrosodimethylamine -D6 (NDMA) from wastewater using model-based techniques. *Journal of Environmental Chemical Engineering*, 6, 4797-4808.

Al-Obaidi M.A., Kara-Zaïtri C., Mujtaba I.M., 2018c. Optimal reverse osmosis network configuration for the rejection of dimethylphenol from wastewater. *J. Environ. Eng*., 144(1), 04017080-1-04017080-9.

Al-Obaidi M.A., Kara-Zaïtri C., Mujtaba I.M., 2018d. Simulation and optimisation of spiral-wound reverse osmosis process for the removal of N-nitrosamine from wastewater. *Chemical Engineering Research and Design*, 133, 168–182.

Bortoluzzi A.C., Faitão J.A., Luccio M.D., Dallago R.M., Steffens J., Zabot G.L., Tres M.V., 2017. Dairy wastewater treatment using integrated membrane systems. *Journal of Environmental Chemical Engineering*, 5, 4819–4827.

Carolin C.F., Kumar P.S., Saravanan A., Joshiba G.J., Naushad Mu., 2017. Efficient techniques for the removal of toxic heavy metals from aquatic environment: A review. *Journal of Environmental Chemical Engineering*, 5, 2782–2799.

Coˆté P., Siverns S., Monti S. 2005. Comparison of membrane-based solutions for water reclamation and desalination. *Desalination* 182, 251-257.

Cristale J., Ramos D.D., Dantas R.F., Junior A.M., Lacorte S., Sans C., Esplugas S., 2016. Can activated sludge treatments and advanced oxidation processes remove organophosphorus flame retardants?. *Environmental Research,* 144, 11–18.

Czech B., Buda W., 2015. Photocatalytic treatment of pharmaceutical wastewater using new multiwall-carbon nanotubes/TiO_2/SiO_2 nanocomposites. *Environmental Research,* 137, 176–184.

Edgar T. F., Himmelblau D. M., Lasdon L. S., 2001. Optimization of chemical processes. McGraw-Hill.

El-Emam R.S., Dincer I., 2014. Thermodynamic and thermoeconomic analyses of seawater reverse osmosis desalination plant with energy recovery. *Energy*, 64, 154-163.

Franks R.N., Bartels C.R., Frenkel V.S., Birch, D., 2012. Evaluating the economics of a unique hybrid RO design after three years of treating brackish groundwater. Hydranautics/Nitto Denko.

Gholami M., Mirzaei R., Kalantary R.R., Sabzali A., Gatei F., 2012. Performance evaluation of reverse osmosis technology for selected antibiotics removal from synthetic pharmaceutical wastewater. *Iranian Journal of Environmental Health Science and Engineering,* 9(1), 19.

George J.S., Ramos A., Shipley H.J., 2015. Tanning facility wastewater treatment: Analysis of physical–chemical and reverse osmosis methods. *Journal of Environmental Chemical Engineering*, 3, 969–976.

Greenlee L.F., Lawler D.F., Freeman B.D., Marrot B., Moulin P., 2009. Reverse osmosis desalination: water sources, technology, and today's challenges. *Water Res*., 43(9), 2317-2348.

Jiang S., Li Y., Ladewig B.P., 2017. A review of reverse osmosis membrane fouling and control strategies. *Science of the Total Environment*, 595, 567–583.

Koroneos C., Dompros A., Roumbas G., 2007. Renewable energy driven desalination systems modelling. *Journal of Cleaner Production*, 15, 449-464.

Lee S., Lueptow, R.M., 2001. Rotating reverse osmosis: a dynamic model for flux and rejection. *Journal of Membrane Science,* 192(1–2), 129–143.

Lu Y.-y., Hu Y.-d., Xu D.-m., Wu L.-y., 2006. Optimum design of reverse osmosis seawater desalination system considering membrane cleaning and replacing. *Journal of Membrane Science*, 282, 7-13.

Lu Y., Liao A., Hu Y., 2012. The design of reverse osmosis systems with multiple-feed and multiple-product. *Desalination*, 307, 42-50.

MacHarg J., Truby R., 2004. West Coast researchers seek to demonstrate SWRO affordability. *Desalination and Water Reuse Quarterly*, 14(3) 1-18.

Madaeni S.S., Koocheki S., 2006. Application of taguchi method in the optimisation of wastewater treatment using spiral-wound reverse osmosis element. *Chemical Engineering Journal*, 119, 37-44.

Malek A., Hawlader M.N.A., Ho J.C., 1996. Design and economics of RO seawater desalination. *Desalination*, 105, 245-261.

Marcovecchio M.G., Aguirre P.A., Scenna N.J., 2005. Global optimal design of reverse osmosis networks for seawater desalination: modeling and algorithm. *Desalination*, 184, 259-271.

Patroklou G., Mujtaba I.M., 2014. Economic optimisation of seawater reverse osmosis desalination with boron rejection. Proceeding of the 24th European Symposium on Computer Aided Process Engineering- ESCAPE 24.

Process System Enterprise Ltd. gPROMS Introductory User Guide. London: Process System Enterprise Ltd., 2001.

Sassi K.M., 2012. Optimal scheduling, design, operation and control of reverse osmosis based desalination. Ph.D. thesis, University of Bradford, UK.

Sassi K.M., Mujtaba I.M., 2013. Optimal operation of RO system with daily variation of freshwater demand and seawater temperature. *Computers and Chemical Engineering*, 59, 101– 110.

Sundaramoorthy S., Srinivasan G., Murthy D.V.R., 2011. An analytical model for spiral wound reverse osmosis membrane modules: Part II – Experimental validation. *Desalination*, 277, 257-264.

Uribe I.O., Mosquera-Corral A., Rodicio J.L., Esplugas S., 2015. Advanced technologies for water treatment and reuse. *AIChE Journal*, 61(10), 3146–3158.

Valladares Linares R., Li Z., Yangali-Quintanilla V., Ghaffour N., Amy G., Leiknes T., Vrouwenvelder J. S., 2016. Life cycle cost of a hybrid forward osmosis e low pressure reverse osmosis system for seawater desalination and wastewater recovery. *Water Research*, 88, 225–234.

Wilf M., 2004. Fundamentals of RO–NF technology. *In Proceedings of International Conference on Desalination Costing*, Limassol, Cyprus, December.

Appendix A

Table A.1. The mathematical modelling of an individual spiral-wound RO system of Al-Obaidi *et al.* (2018c)

Model Equations	Specifications	Eq. no.
$J_w = A_w \left[\left(\frac{\left(P_{f(in)}+P_{f(out)}\right)}{2} - P_p\right) - \left(R\,(T+273.15)\,(C_w - C_p)\right)\right]$	The permeate flux (m/s)	1
$J_s = B_s\,(C_w - C_p)$	The solute flux (kmol/m² s)	2
$\frac{(C_w - C_p)}{(C_b - C_p)} = exp\left(\frac{J_w}{k}\right)$	The wall solute concentration (kmol/m³)	3
$k = \frac{147.4\,D_b\,Re_f^{0.13}\;Re_p^{0.739}\,C_m^{0.135}}{2\,t_f}$	The mass transfer coefficient (m/s) of chlorophenol (Sundaramoorthy et al., 2011)	4
$C_m = \frac{C_b}{\rho_w}$	The dimensionless solute concentration (dimensionless)	5
$D_b = 6.725E-6\;exp\left\{0.1546E-3(C_f\,x18.0125) - \frac{2513}{(T+273.15)}\right\}$	The diffusivity parameter at the feed channel (m²/s) (Koroneos, 2007)	6
$D_p = 6.725E-6\;exp\left\{0.1546E-3(C_p\,x18.0125) - \frac{2513}{(T+273.15)}\right\}$	The diffusivity parameter at the permeate channel (m²/s)	7
$\mu_b = 1.234E-6\,exp\left\{0.0212\,(C_f\,x18.0153) + \frac{1965}{(T+273.15)}\right\}$	The dynamic viscosity (kg/m s) at the feed channel	8
$\mu_p = 1.234E-6\,exp\left\{0.0212\,(C_p\,x18.0153) + \frac{1965}{(T+273.15)}\right\}$	The dynamic viscosity (kg/m s) at the permeate channel	9
$\rho_b = 498.4\,m_f + \sqrt{\left[248400\,m_f^2 + 752.4\,m_f\,C_f\,x18.01253\right]}$	The feed density (kg/m³)	10
$\rho_p = 498.4\,m_f + \sqrt{\left[248400\,m_f^2 + 752.4\,m_f\,C_p\,x18.01253\right]}$	The permeate density (kg/m³)	11
$m_f = 1.0069 - 2.757x10^{-4}\,(T)$	Parameter in Eqs. (10) and (11)	12
$Re_f = \frac{\rho_b\;de_b\,Q_b}{t_f\,W\,\mu_b}$	The Reynolds number at the feed channel (dimensionless)	13
$Re_p = \frac{\rho_p\;de_p\;J_w}{\mu_p}$	The Reynolds number at the permeate channel (dimensionless)	14
$de_b = 2t_f \qquad de_p = 2t_p$	The equivalent diameters of the feed and permeate channels (m)	15
$U_b = \frac{Q_b}{W\,t_f}$	The bulk feed velocity (m/s)	16
$Q_b = \frac{Q_f + Q_r}{2}$	The bulk feed flow rate (m³/s)	17
$C_b = \frac{C_f + C_r}{2}$	The bulk concentration (kmol/m³)	18
$C_p = \frac{C_f\,B_s}{\left(\frac{J_w}{\exp(\frac{J_w}{k})} + B_s\right)}$	The permeate solute concentration (kmol/m³)	19
$Q_f = Q_r + Q_p$	The retentate flow rate (m³/s)	20
$Q_f\,C_f = Q_r\,C_r + Q_p\,C_p$	The retentate concentration (kmol/m³)	21
$Q_p = J_w\,A$	The total permeated flow rate (m³/s)	22

Table A.1. The mathematical modelling of an individual spiral-wound RO system of Al-Obaidi *et al.* (2018c) (Continued)

Model Equations	Specifications	Eq. no.
$P_{f(out)} = P_{f(in)} - \frac{bL}{\emptyset \sinh \emptyset}\{(Q_f + Q_r)(cosh\emptyset - 1)\}$	The retentate pressure (Sundaramoorthy et al., 2011)	23
$\emptyset = L\sqrt{\frac{W\ b\ A_W}{\left[1+\left(\frac{A_W\ R\ C_p\ (T+273.15)}{B_S}\right)\right]}}$	Parameter in Eq. (23)	24
$\Delta P_{f(in)} = P_{f(in)} - P_p$	The pressure difference at the inlet edge (atm)	25
$\Delta P_{f(out)} = P_{f(out)} - P_p$	The pressure difference at the outlet edge (atm)	26
$Rec = \frac{Q_p}{Q_f}$	The total permeate recovery (dimensionless)	27
$Rej = \frac{C_f - C_p}{C_f}$	The solute rejection (dimensionless)	28
$E = \frac{\left(\left(P_{f(in)}\ x101325\right) Q_f\ \right)}{\frac{Q_p\ \varepsilon_{pump}}{36x10^5}}$	The specific consumption energy of HPP (kWh/m³)	29

Highlights

1. Retentate-permeate reprocessing design improved the rejection with energy saving.

2. Increasing operating temperature or pressure can reduce the product unit cost.

3. A reduction in total annual cost is noted due to increase the feed concentration.

4. A max. chlorophenol rejection of 98.8% at approximately 0.21 $/m³ can be achieved.

5. Increasing feed concentration is worthy to reduce some of operating cost factors.